

POSTBUCKLING BEHAVIOUR OF A STIFFENED PANEL SUBJECT TO COMBINED LOADING

Carol A. Featherston*, Konan Koffi** and Richard Burguete**

*Cardiff School of Engineering, Queen's Buildings, The Parade, Cardiff, CF24 3AA, UK.

**Airbus UK, New Filton House, Filton, Bristol, BS99 7AR, UK.

Keywords: *Postbuckling, stiffened panel, shear, in-plane bending, FEA.*

Abstract

Aircraft wing spars comprise stiffened panels loaded under a combination of shear, compression and in-plane bending, which are subject to failure by buckling. Due to the redistribution of stresses into the stiffeners after initial buckling of the plates which constitute these panels the structure has significant load carrying capability in the postbuckling region. Through experimental studies of both initial buckling and the early stages of postbuckling, the paper examines this load transfer and the corresponding stiffness behaviour, and looks at the use of nonlinear finite element techniques to predict this behaviour.

1 Introduction

A continuing need to exploit the structural reserves of aircraft assemblies such as the wings and fuselage has placed increased importance on the accurate prediction of their behaviour at high loads. Many such structures comprise thin walled shells subject to potential failure due to instability. A number of these structures however buckle in a stable manner and have significant load carrying capability in the postbuckling region. It is essential that this capability can be quantified, thereby allowing the design envelope to be extended into this region, leading to significant weight reduction and hence cost benefits.

One such structure of interest is the wing spar, which provides one of the main load paths for vertical shear loading, and which is also subject to compression and in-plane bending due to

wing bending. This structure comprises a panel stiffened both horizontally and vertically, with the stiffeners having the effect of dividing the panel up into a number of smaller plates which provides two advantages. Firstly, the initial local buckling load of each of the constituent plates is greater than that of a much larger plate subject to the same loading, and secondly load redistribution to the stiffeners following local buckling (of these plates) provides extensive postbuckling load carrying capacity.

The buckling failure of such structures under pure shear, with the development of either a complete or incomplete tension field providing load carrying capability in the postbuckling region, is relatively well understood and is documented along with other simplified load cases in a number of texts (e.g.[1]) and used in design guides such as ESDU [2]. In many cases however, for the purpose of design, the role of the stiffeners is reduced to that of providing either simple support or clamped boundary conditions (depending on geometry) to a series of plates which can then be designed to avoid initial buckling. Some work has been carried out to examine further the contribution of the stiffeners for relatively simple designs [3]. However for structures with more complex geometries and loading cases, it is necessary to use tools such as finite element analysis in order to provide a more detailed analysis of the full buckling and postbuckling behaviour. That given, questions still arise as to the best way to model real structures in the absence of exact geometric information, as is normally the case at the design stage.

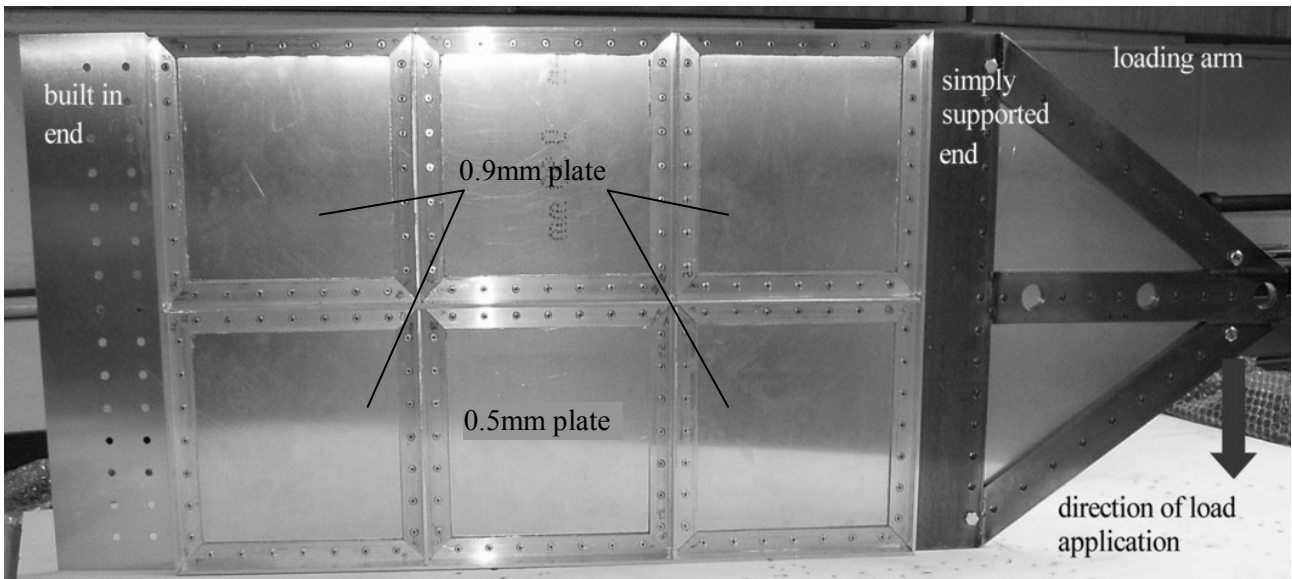


Fig. 1 Test Specimen

This paper describes an experiment in which a stiffened panel built-in at one end and simply supported at the other is loaded in-plane to produce a combination of shear, compressive and in-plane bending stresses. The results of these tests are compared with those obtained by modelling the structure using finite element analysis in order to determine the suitability of this technique.

2 Experimental Set-up

2.1 Specimen

The test specimen was designed to represent a simplified wing spar 600mm long by 400mm high, divided by a series of stiffeners into six plates 200mm x 200mm. It was constructed

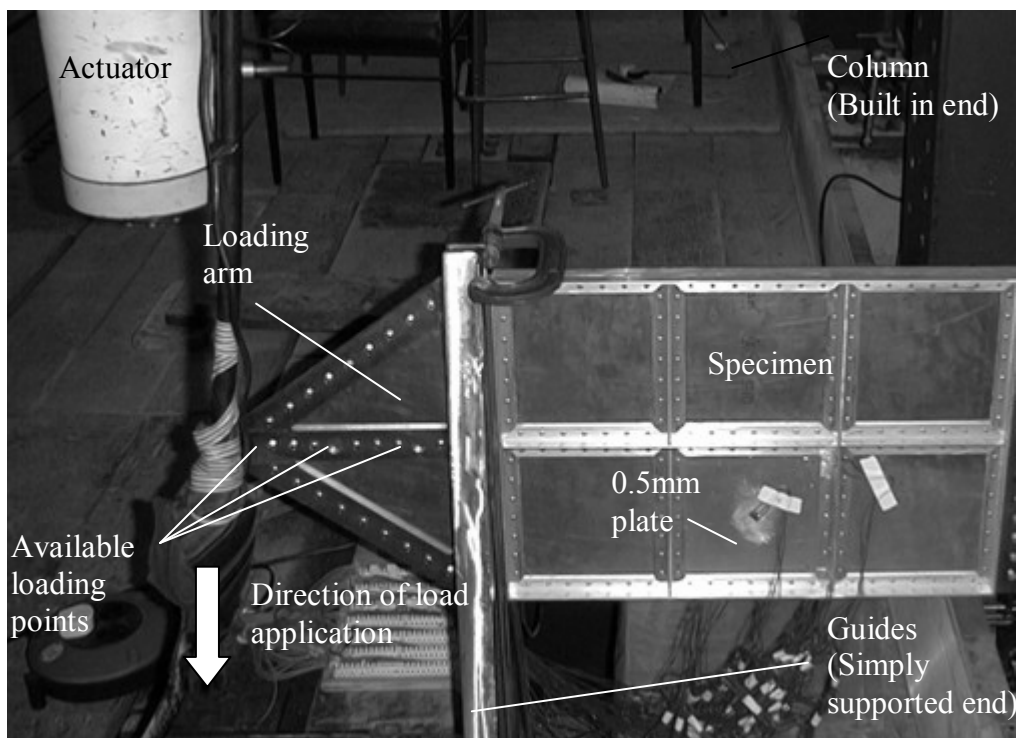


Fig. 2 Experimental Set-up

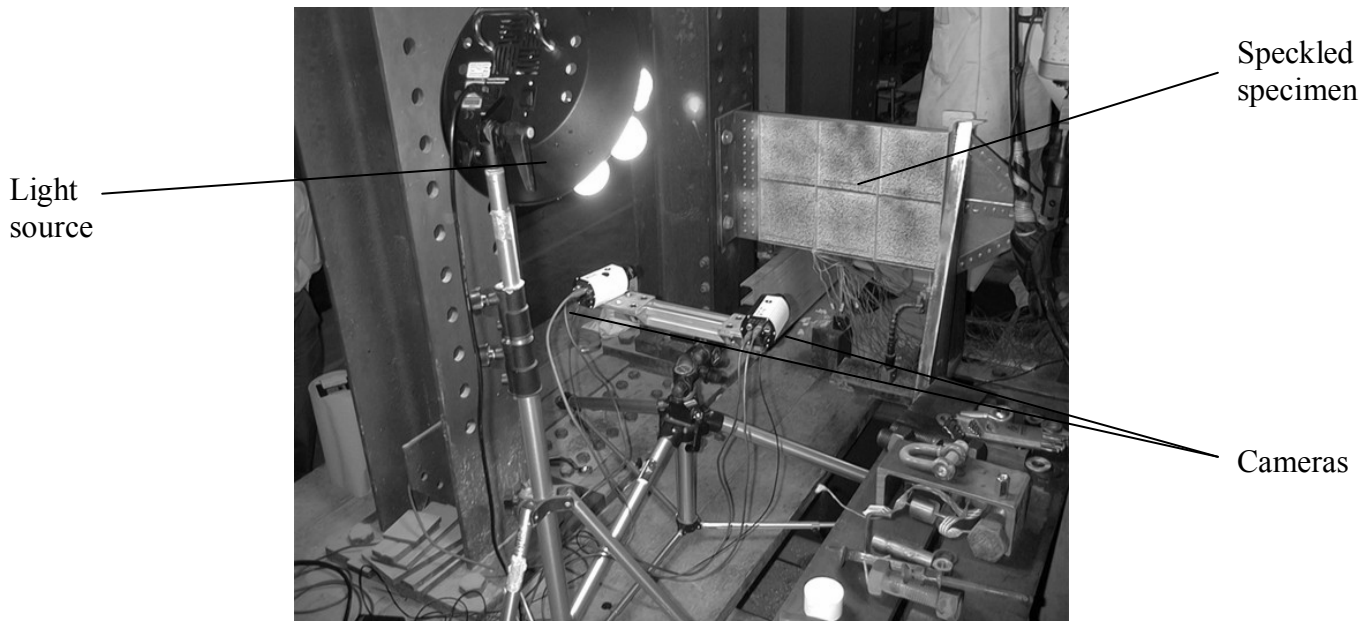


Fig. 3 Full Field Image Correlation

mainly from 0.9mm thick aircraft grade duraluminium (BS1470 6082 – T6), with a reduced thickness plate (see Figure 1) of 0.5mm inset, to encourage buckling in the central lower plate, in which boundary effects would be minimal.

The panel was stiffened on both sides using 3.2mm thick extruded duraluminium sections, with a web height and individual flange width of 19mm (giving an overall width of 38mm for the T-section stiffeners (Figure 1)). These were attached using a combination of adhesive (Loctite Multibond 330 with 7387 activator) and 3.2mm pop rivets (spaced 25mm apart).

Finally, to allow the attachment brackets and loading mechanism to be bolted through the specimen to aid load transfer, the ends of the panel were extended beyond the stiffeners

2.2 Test Rig

The specimen was tested using an adaptable test frame consisting of a floor, a number of moveable I beam columns drilled through their flanges at regular intervals to allow additional sections/brackets etc to be bolted on, and a series of moveable cross pieces also drilled to allow the attachment of actuators or further supports. This frame can be set up relatively

easily to test a wide range of different shapes and sizes of structures (maximum capacity approximately 3m x 3m x 12m), subject to a variety of single or combination loads depending on the actuators selected.

The test panel was attached to one of the upright columns using a pair of specially designed brackets bolted through the specimen using a total of thirty 6mm diameter bolts, arranged in two vertical lines (Figure 1). The aim of this set-up was to provide built-in end conditions, ensuring no sliding or rotation of the specimen relative to the frame occurred during the test. At the other end of the panel, two load applicators were again bolted through its thickness, using a further series of 6mm diameter bolts (Figure 2). In addition to ensuring an even load application with minimal localised effects, these load applicators provided a number of loading attachment points, thereby allowing several different combinations of shear and compressive load to be introduced by changing the moment arm and thus increasing or decreasing in-plane bending whilst maintaining the same degree of shear. For the purposes of this test however, only one loading point was utilised – that giving the greatest in-plane bending to shear ratio possible.

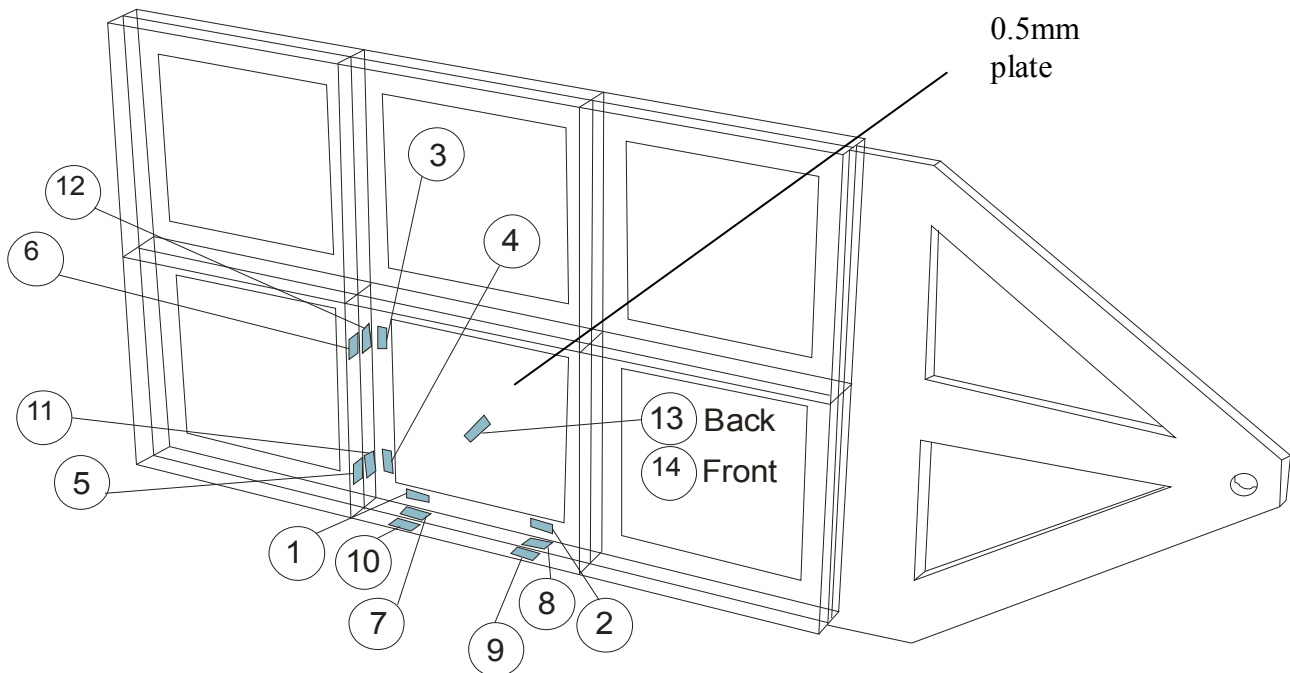


Fig 4 Strain Gauge Positioning

Loading was applied using a 250kN Dartec actuator fitted with a 5kN load cell, operated under displacement control. The actuator was driven at a rate of 0.001 mm/s until the load reached 5kN.

Finally, in order to provide the simply supported edge conditions along the vertical edge of the panel closest to the point of loading, the structure and the loading arms were constrained to move between a pair of guides, which were in turn bolted to the floor of the test frame. These allowed translation in the vertical and horizontal directions, but no movement out of plane.

2.3 Instrumentation

Load, displacement and strain were monitored at a series of points across the specimen throughout the testing process. Load was measured using the load cell and recorded using a Schlumberger SI 3531D data acquisition system. Both in-plane displacement at the point of loading and out-of-plane displacement in the centre of the reduced thickness plate were also monitored using 0-10mm LVDT's and the data recorded using the same system as for the load. Full-field in and

out-of-plane-displacement, and in-plane strain measurements were also made using the VIC 3D image correlation system (Figure 3). This uses white light to illuminate the surface of the specimen onto which is painted a speckle pattern. During deformation the grey scale pattern in each of a series of small areas covering the specimen is tracked to establish its motion. This allows the position and through further processing, the surface strain at a number of points on the specimen to be established.

Due to the set-up of the image-correlation equipment it was not possible to determine the strains in the stiffeners. The strains in the flanges and the webs of the stiffeners and in the centre of the thin plate were therefore monitored using a series of Vishay CEA-06-120CZ-120 rectangular rosette strain gauges again connected to the data acquisition system. The positions of the strain gauges are illustrated in Figure 4. As can be seen the gauges were limited to one horizontal and one vertical stiffener which were selected as those having the greatest change in strain during the loading process, based on the results of preliminary finite element analyses. The position of each strain gauge with respect to the

stiffener was also selected to correspond to the area of maximum strain using the results of the finite element analysis.

3 Finite Element Analysis

3.1 Model

Following convergence tests, the panel was modelled using elements with an average edge length of 5mm. The main plates and stiffeners were modelled using quadrilateral S8R5 (Shell element with 8 nodes, using Reduced integration and having 5 degrees of freedom per node) elements which behave in a manner consistent with thin shell theory, and the loading arms were modelled using 10 noded tetrahedral elements for compatibility with the shell elements at the interface.

At the 'built-in' end of the structure five degrees of freedom were restricted, with rotation about the vertical axis enabled. At the simply supported end, the plate was prevented from moving or rotating out of plane along a line corresponding to the vertical supports.

Load was applied across a number of nodes in the loading eyelet to prevent stress concentration effects.

Fully nonlinear material models were used throughout, with material properties based on the results of earlier experimental work [6].

3.2 Linear Eigenvalue Analysis

To obtain the mode shapes necessary to model geometric imperfections in the fully nonlinear analysis, an eigenmode analysis based on a linear perturbation procedure was performed. In this procedure a stiffness matrix corresponding to the base state loading on the structure is initially stored prior to a small perturbation or live load being applied. In this particular case the base state is the unloaded condition and the matrix used is the original stiffness matrix \mathbf{K}_0 . The program derives the initial stress matrix due to the live load (\mathbf{K}_p) and an eigenvalue calculation is performed to determine a multiplier (λ) to the live load at which the structure becomes unstable:

$$[\mathbf{K}_0 + \lambda\mathbf{K}_p]\phi = 0 \quad (1)$$

where ϕ represents the eigenmode corresponding to each eigenvalue. Subspace iteration is used for eigenvalue extraction, thereby allowing several modes to be calculated simultaneously. In this study a total of twelve eigenvalues were calculated, to ensure all the eigenmodes likely to occur within the loading range were found.

3.3 Nonlinear / Imperfection Sensitivity Analysis

Once the mode shapes had been calculated, these were used to model imperfections which were then incorporated into the 'perfect geometry' of the original model prior to carrying out a fully nonlinear analysis to predict the buckling load and postbuckling behaviour of the panel. This was done using the Riks method which uses non-linear static equilibrium equations to solve unstable problems, where the load-displacement response is such that either the load or the displacement may decrease as the solution evolves. A number of studies were performed on geometries with a range of imperfections having amplitudes based on the maximum geometric imperfection measured in the test specimen. These imperfections were based on both single eigenmodes and combinations of several eigenmodes, in order to begin to investigate the best possible method for obtaining a lower limit for the postbuckling behaviour of such a structure, in the absence of information on exact geometry, in order to accurately represent the problems facing the design engineer.

4 Results and Discussion

The overall buckling and early postbuckling behaviour (up to over four times the initial buckling load) can be seen in Figure 5, where the out-of-plane displacement of the centre of the thinnest plate is plotted against load, illustrated by a series of experimentally determined full-field out-of-plane displacement

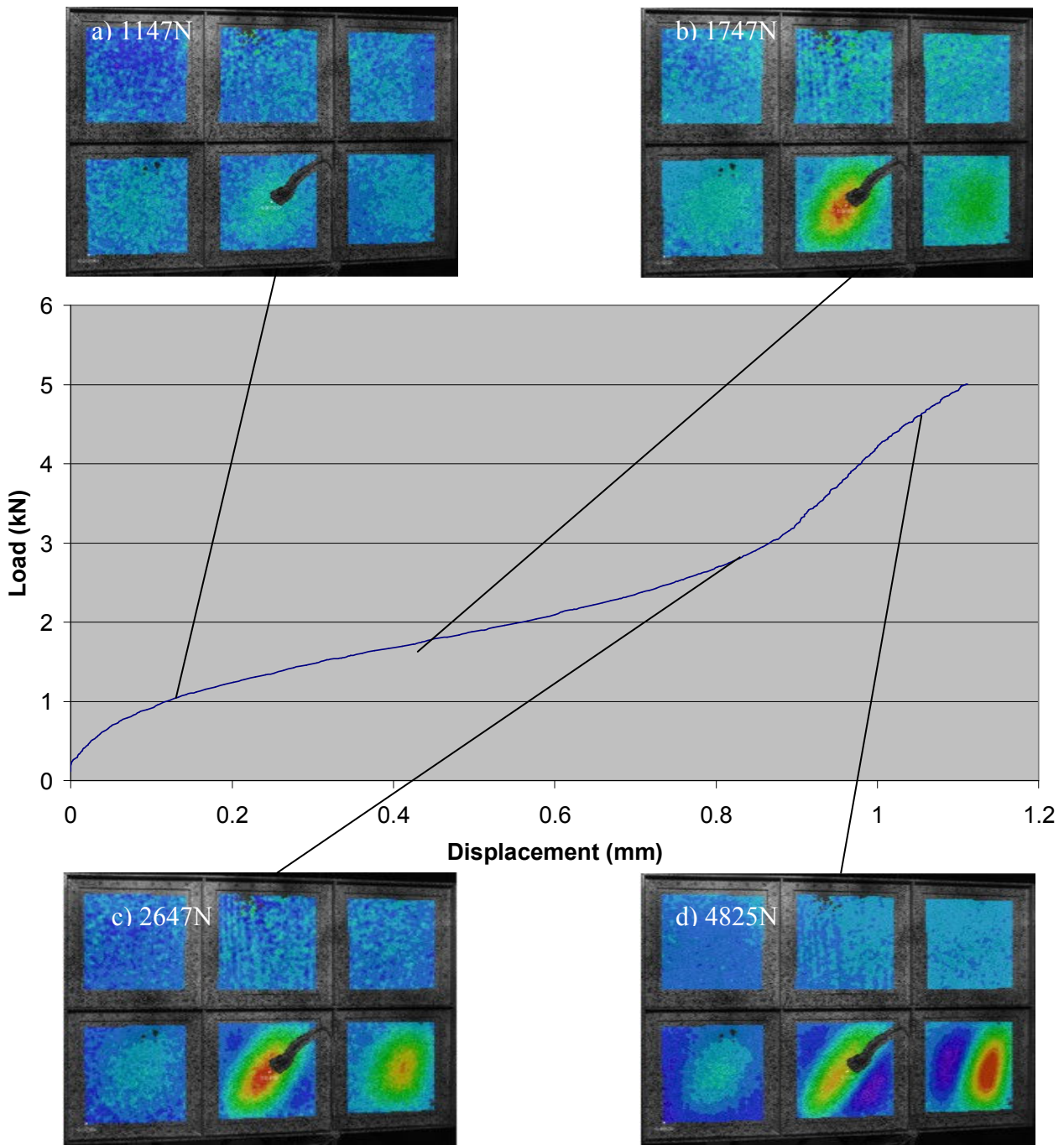


Fig. 5 Load versus Out-of-Plane Displacement (Full Field)

plots at four key points during the loading process. Following initial buckling of the central lower plate at 960N (calculated by taking the intersection of tangents to the pre and post buckling gradients, and confirmed by the results from strain gauges 13 and 14) the structure is (as expected) stable, maintaining an increasing load capacity, though at a reduced rate. This continues up to a load of

approximately 2kN with the shape of the eigenmode developing due to the increase in load and two further lobes appearing in the lower central plate (Figure 5b). As the load approaches 2kN, a buckle develops in the bottom right hand plate, which is in fact the most heavily loaded part of the structure (Figure 5c). This also develops to form two lobes whose orientation reflects the

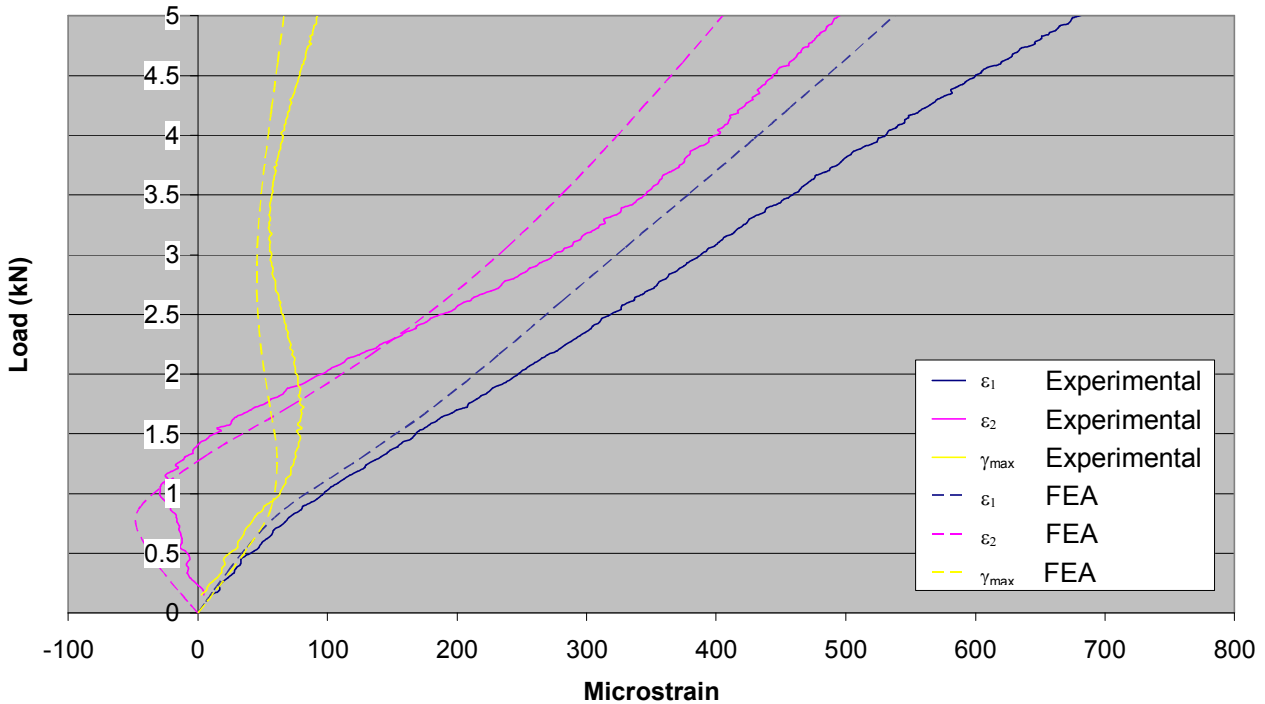


Fig. 6 Load versus Strain for Strain Gauge 13

increased ratio of compressive to shear load in the plate due to the greater bending stress resulting from the increased moment arm further away from the point of loading (Figure 5d). The buckling of this plate is accompanied by an increase in the stiffness of the overall panel as the first lobe develops and a slight decrease with the appearance of the second. By the end of the test, the panel has been loaded to over four times the initial buckling load whilst still maintaining stable behaviour.

The proportion of the load carried by the central lower plate at each stage can be determined by examination of Figure 6, which presents the results obtained from strain gauge 13 positioned at the centre of the reverse side of the plate (Figure 4). Of particular note is the plot of γ_{\max} against load which clearly indicates the increasing shear load carried by the plate up to and slightly after the initial buckling point which then drops off shortly afterwards only to begin to build up again later after around the 3kN point.

The development of the tension field which allows not only the overall structure, but also

the buckled plates themselves to carry this increased load and progress to higher buckling modes can be clearly seen in Figure 7, which presents the results of the finite element analysis work in terms of both principal strain (ϵ_1) and stress (von Mises) distribution at key points throughout the buckling and postbuckling process. In the first pair of images, taken just into the postbuckling range at a load of 1834N the tension field can be seen to be starting to develop, creating regions of high strain in the stiffeners, and in particular, in the horizontal stiffeners. In the second set of contours, representing the situation well into the postbuckled range, this field can be seen to be much further developed with the corresponding increases in strain, again mainly in the horizontal stiffeners, but with some presence in the adjacent vertical ones. Finally at a load of 5194N and therefore at a slightly higher load than that applied during the test, a second tension field develops in the lower right hand plate, again in particular increasing the strain in the horizontal stiffeners.

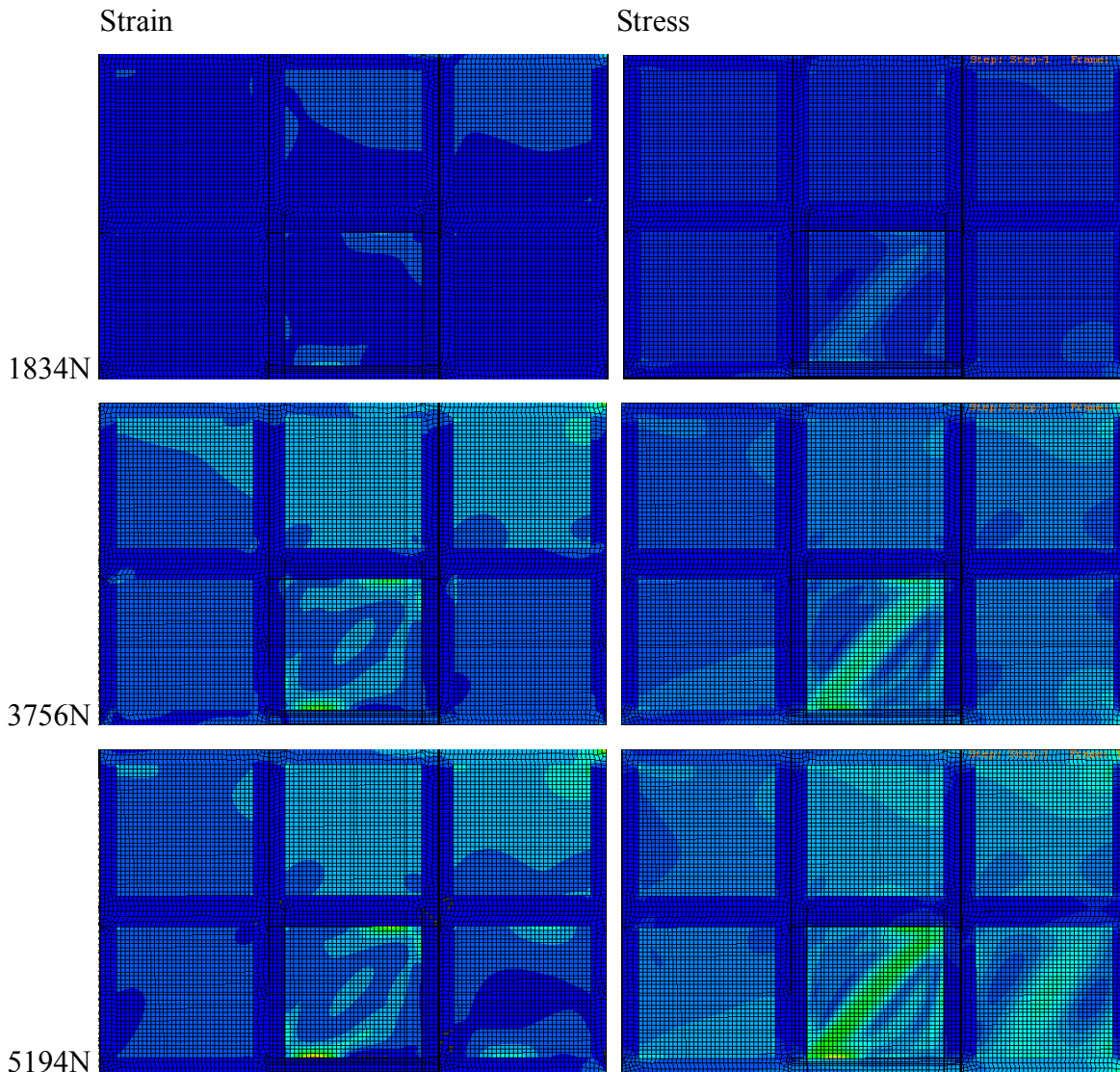


Fig. 7 Tension Field Development

The transfer of load into the stiffeners required to set up the tension field is illustrated in Figure 8, which plots shear load in the rear vertical stiffener monitored by strain gauge 12 against strain. (Due to the uneven distribution of load transferred into the stiffeners which can be seen by reference to Figure 7, gauges 6 and 12, and 8 and 9 show the effects of this load transfer more markedly. The results presented for gauge 12 are typical of those found for each of these gauges.) Clearly, in the period prior to buckling, very little strain is experienced by the stiffener, and the load is carried in the plate (in this case the central lower plate). As the

buckling point is reached, the strain, and therefore the load carried by the stiffener, increases significantly. As the load approaches 4kN there is a further marked increase in the strain in the stiffener, which is believed to be associated with the development of the tension field in the lower right hand plate which also relies on increasing the load transferred to this particular stiffener.

As previously stated, one of the main purposes of this study was to examine the suitability of nonlinear finite element analysis to predict the postbuckling behaviour of such a panel. For single plates, even those under complex load

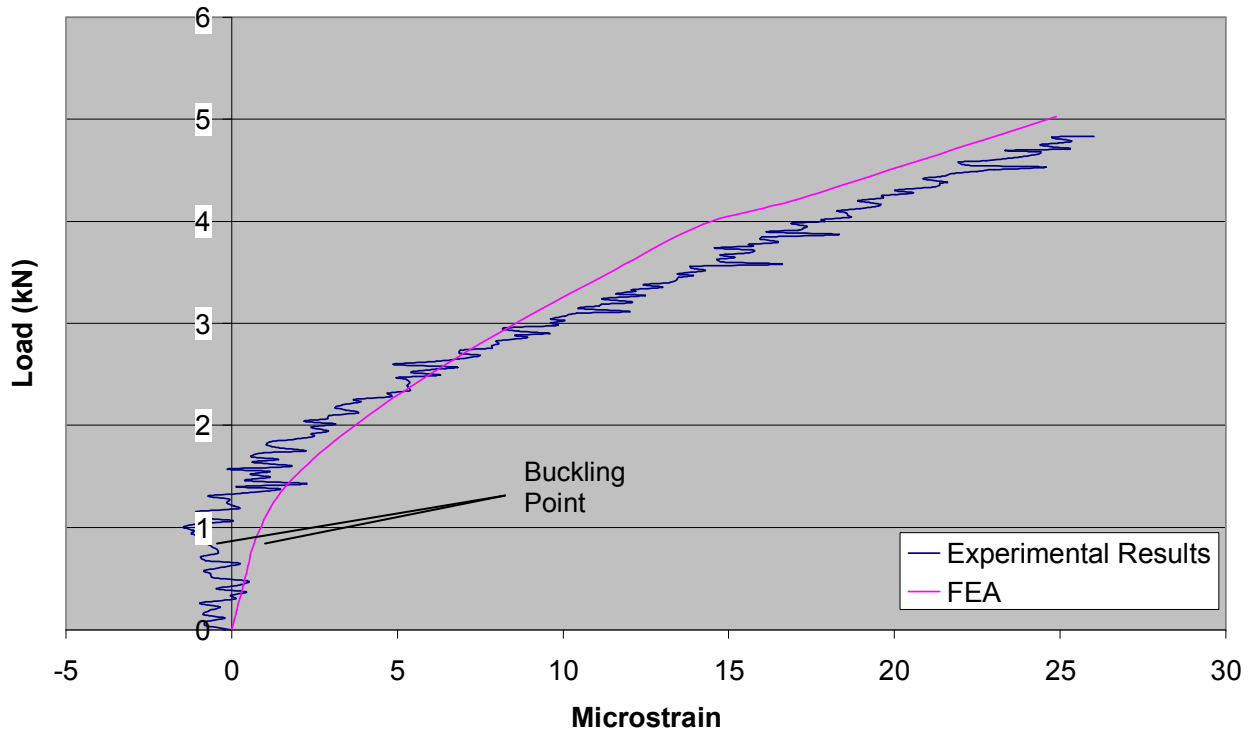


Fig. 8 Load versus Shear Strain for Strain Gauge 12

and boundary conditions, nonlinear analyses based on perfect structures modified by the addition of imperfections in the form of the first few eigenmodes as suggested by Speicher and Saal [4] have been used successfully to provide a lower limit to buckling and postbuckling performance [5,6]. However for more complex structures in which interactions between many possible local and overall eigenmodes could occur, much less evidence of this suitability exists. Figure 9 shows the results of a number of nonlinear analyses based on a perfect panel with imperfections in the form of the first eigenmode, combinations of eigenmodes which appear during experimental work to be significant (in this case 1&5), all eigenmodes which occur up to the buckling point and all eigenmodes weighted such that the first has the largest amplitude, and the remainder are scaled according to:

$$\text{Max amplitude of mode of interest} = 0.05 \times \frac{\text{Eigenvalue corresponding to mode one}}{\text{Eigenvalue corresponding to mode of interest}} \quad (2)$$

In each case the maximum amplitude introduced was 0.05mm which represented the maximum imperfection found during initial studies of the geometry of the specimen. Inspection of the results shows that even for this more complex problem, studies based on the introduction of an imperfection in the form of the first eigenmode, scaled to have a maximum amplitude equal to that of any anticipated defects provides excellent agreement up to in excess of twice the buckling load, and thereafter is conservative and therefore suitable for use in design. It is of interest to note that the introduction of further eigenmodes can be seen to actually increase the initial stiffness, thereby overestimating the behaviour of the structure throughout the buckling and postbuckling range. It is thought that this may be due to the imperfections introduced encouraging the structure to ‘jump’ straight to one of the higher eigenmodes, missing the first and therefore overestimating the initial and early postbuckling stiffness. In any event, it seems that for early postbuckling,

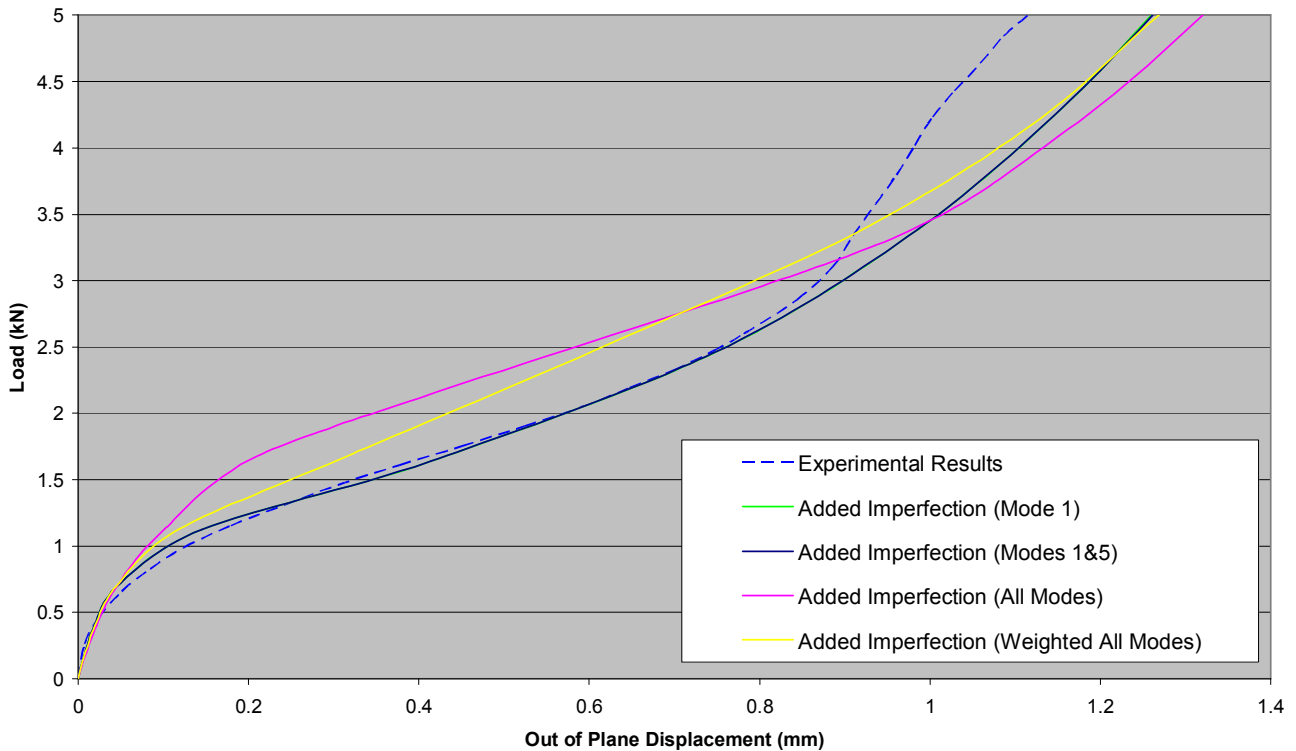


Fig. 9 Imperfection Sensitivity

this level of complexity is not necessary to obtain a useful model for design.

5 Conclusions

An experiment has been performed to examine the buckling and postbuckling behaviour of a stiffened panel, and in particular the transfer of load from the plates constituting this panel into the stiffeners at higher loads. The structure has been seen to behave in a stable manner in the postbuckling period, and has been shown to be capable of supporting loads in excess of four times the initial buckling load. Moreover, a relatively simple nonlinear finite element analysis has been shown to accurately predict this behaviour at up to twice the initial buckling load, being conservative thereafter.

Acknowledgements

The authors acknowledge the contributions made by Mr S Tapfield, Mr T Crook, Mr K Htut, Mr S Mead, Mr L Czekaj, Mr D Sandford, Mr B Hooper and in particular Mr O Montury, to this work.

References

- [1] Gerard G and Becker H. *Handbook of Structural Stability, Pt.I, Buckling of Flat Plates*, NACA Tech. Note 3781, 1957.
- [2] Engineering Sciences Data Unit (ESDU), Flat Panels in Shear. Buckling of Long Panels with Transverse Stiffeners. *ESDU 02.03.02*, 1971.
- [3] Featherston C A, Kennedy D, Weston D J and Koffi K. Design Rules for Panel Buckling Under Combined Shear, Compression and Bending, *Fourth International Conference on Thin-Walled Structures*, Loughborough University, pp 153-160, 2004.
- [4] Speicher G and Saal H. Numerical calculation of limit loads for shells of revolution with particular regard to the applying equivalent initial imperfection, *Buckling of Shell Structures, on Land, In the Sea, and in the Air*, Elsevier Applied Science, London, pp 466-475, 1991.
- [5] Featherston C A and Ruiz C. Buckling of Flat Plates under Bending and Shear, *Journal of Mechanical Engineering Science Proceedings Part C*, Vol. 212, pp 249-261, 1998.
- [6] Featherston C A and Ruiz C. Buckling of Curved Panels under Combined Shear and Bending, *Journal of Mechanical Engineering Science Proceedings Part C*, Vol. 212, pp 183-196, 1998.